Landscape Ecology **15:** 679–695, 2000.

Physico-chemical heterogeneity in a glacial riverscape

Florian Malard*, Klement Tockner and J. V. Ward
*Department of Limnology, EAWAG/ETH, Ueberlandstrasse 133 CH-8600 Duebendorf, Switzerland; *(Corresponding author: Present address: Florian Malard Hydrobiologie et Ecologie Souterraines, ESA CNRS 5023, Université Claude Bernard, Lyon 1, Bat. 403, 43 Bd du 11 Novembre 1918, F-69622 Villeurbanne Cedex, France, Fax: (33) 4 72 43 15 23 E-mail: malard@univ-lyon1.fr)*

Received 4 May 1999; Revised 24 March 2000; Accepted 5 June 2000

Key words: flow path, flood pulse, glacial river, hydrological connectivity, riverscape heterogeneity, water chemistry, water source

Abstract

Spatio-temporal heterogeneity in physico-chemical conditions associated with the annual expansion/contraction cycle in a complex glacial flood plain of the Swiss Alps was investigated employing a landscape approach. The diverse and dynamic aquatic habitats of the flood plain were visualized as an aquatic mosaic or riverscape. Based on samples collected at ca. monthly intervals for 1.5 yr along 17 floodplain transects, the 3 components of riverscape heterogeneity, extent, composition, and configuration, were quantified using categorical maps and indices of landscape patterns for turbidity and specific conductance. Changes in the spatial heterogeneity of 13 other physico-chemical parameters were further analyzed by means of a within-dates principal component analysis. Riverscape heterogeneity (RH), quantified by applying several indices of landscape pattern to turbidity and specific conductance data, was minimum during groundwater-dominated base flow in winter. Despite an increase in surface connectivity in the channel network with rising discharge, RH rose in spring and summer as additional chemically-distinct water sources (i.e., snowmelt runoff and glacial ablation) contributed to surface flow within the flood plain. Most other physico-chemical variables measured during this study exhibited the same spatio-temporal heterogeneity as turbidity and specific conductance. Overall, the glacial flood plain shifted from a monotonous physico-chemical riverscape in winter to a complex mosaic in summer, this seasonal pattern being clearly driven by hydrological factors operating at the catchment scale rather than by autogenic processes within individual water bodies. Although RH exhibited a predictable annual pattern in response to the seasonal flow regime, we expect the channel network to undergo future modifications from stochastic factors associated with flood events and long-term changes reflecting movements of the glaciers.

Introduction

River-floodplain systems as defined by Junk et al. (1989) comprise a variety of permanent aquatic habitats (e.g., main channel, cut-off channels, oxbow lakes) and the floodplain surface, that is the area periodically inundated by the lateral overflow of the river. Natural river-floodplain systems are never static, their aquatic habitats are in constant temporal and spatial change. Non-erosive flooding temporarily modifies environmental conditions in pre-existing water bodies and increases the extent of ephemeral aquatic habitats, while erosive floods can rejuvenate, create, or eliminate water bodies (Bayley 1995; Ward 1997). Thus, from a landscape perspective (Turner and Gardner 1991; Wiens 1995), the different aquatic habitats of river-floodplain systems form a spatially heterogeneous area, i.e., an aquatic mosaic or riverscape, where physico-chemical characteristics vary through space and time in response to biotic and abiotic processes.

Studies emphasizing physico-chemical heterogeneity of surface water in river-floodplain systems have reported either on seasonal changes of individual water bodies or on differences among various aquatic

habitats during defined hydrological periods. In large, pristine, tropical rivers that show only one predictable flood peak per year, nutrient concentrations in floodplain water bodies vary seasonally depending on the relative contribution of river water and on the strength of autogenic processes (e.g., biological uptake, nutrient release) (Hamilton and Lewis 1987; Forsberg et al. 1988; Furch and Junk 1993). In temperate river-floodplain systems that have a less predictable flow regime and reduced hydrological connectivity due mainly to river regulation, emphasis has been put on chemical variability among floodplain water bodies as a function of water sources (e.g., river water, seepage water, hillslope ground water) (Bornette and Amoros 1991; Trémolières et al. 1993; Van den Brink et al. 1993; Burt and Haycock 1996; Parch et al. 1996; Tockner et al. 1999). Glacial rivers share common hydrological characteristics with other types of river systems. Indeed, they have a distinct seasonal flow regime due to the annual freeze-thaw cycle but they also undergo unpredictable floods in response to rainfall events (Milner and Petts 1994). Although the hydrology and physico-chemical features of glacial rivers have been studied intensively (Gurnell and Clark 1987), we are unaware of any published work reporting on a comprehensive investigation of physico-chemical dynamics in a glacial flood plain.

In a previous study (Ward et al. 1999, Malard et al. 1999), we examined the seasonal changes in the relative contribution of different subcatchment water sources to the flow of surface water within a glacial flood plain of the Swiss Alps (Val Roseg, Switzerland). The present paper is going a step further because it aims to determine the relationships between physico-chemical riverscape heterogeneity and discharge, water sources, channel length and surface hydrological connectivity. We hypothesized that: (1) the physico-chemical mosaic would reflect hydrological factors operating at the catchment scale (i.e., changes in water sources, flow paths and hydrological connectivity) rather than autogenic processes operating within the floodplain water bodies; (2) riverscape heterogeneity would increase with rising discharge in spring but it would decrease during the ablation period in summer as hydrological connectivity between floodplain water bodies becomes maximum. We developed an innovative approach in running water ecology for the quantification of riverscape heterogeneity (RH). First, we used an extensive data set derived from systematic measurements across the channel network to map monthly changes in spatial patterns of turbidity and specific conductance. Second, RH was quantified by applying several indices of landscape pattern to these categorical maps. Third, we related the spatio-temporal patterns of heterogeneity exhibited by 13 other physico-chemical parameters to the seasonal changes in RH calculated from turbidity and specific conductance data.

Materials and methods

Study site

The Roseg River, a 11.5 km long second-order tributary of the River Inn, is situated in the Bernina Massif of the Swiss Alps (Figure 1). The upper catchment of the river was described in detail by Tockner et al. (1997) and Malard et al. (1999). Its area is 49.5 km^2 with elevations ranging from 1990 to 4049 m a.s.l. (mean elevation: 2840 m). Glaciers, exposed crystalline rock, a rock-soil complex supporting herbaceous vegetation, and subalpine forests occupy 42, 35, 19 and 4%, respectively, of the upper catchment. The average annual precipitation is approximately 1.6 m, of which about half is snow (Spreafico et al. 1992).

The floodplain area is 0.67 km^2, 85% of which is covered by unstable gravels with sporadic pioneer plants (dominant species: *Epilobium fleischerii*, *Rumex scutatus*, *Trifolium repens*) or by sparse grass. The upper section of the flood plain (transects 7 to 14 in Figure 1) is steeper (slope: 4.8%) and wider (up to 510 m wide) than the lower section (average slope: 1.9%, width 130–260 m). Based on surface hydrological connectivity with the main channel and source of water, Tockner et al. (1997) identified six distinct channel types in the flood plain: the main channel (code M in Figure 1), side channels (S), intermittently-connected channels (I), mixed channels (X), groundwater channels (G), and tributaries (T). Intermittently-connected channels have a permanent surface connection at their downstream ends but an intermittent surface connection with the main channel at their upstream ends. Mixed channels are fed by two or more water sources: main channel, a side tributary, or groundwater upwelling. Groundwater channels have no upstream connection with surface channels since they are fed by alluvial or hillslope groundwater.

Several hydrological reservoirs contribute to the flow of surface water within the floodplain, thereby inducing a distinct seasonal flow regime (Figure 2). Winter base flow (January–March) is sustained primarily by upwelling of hillslope and deep alluvial

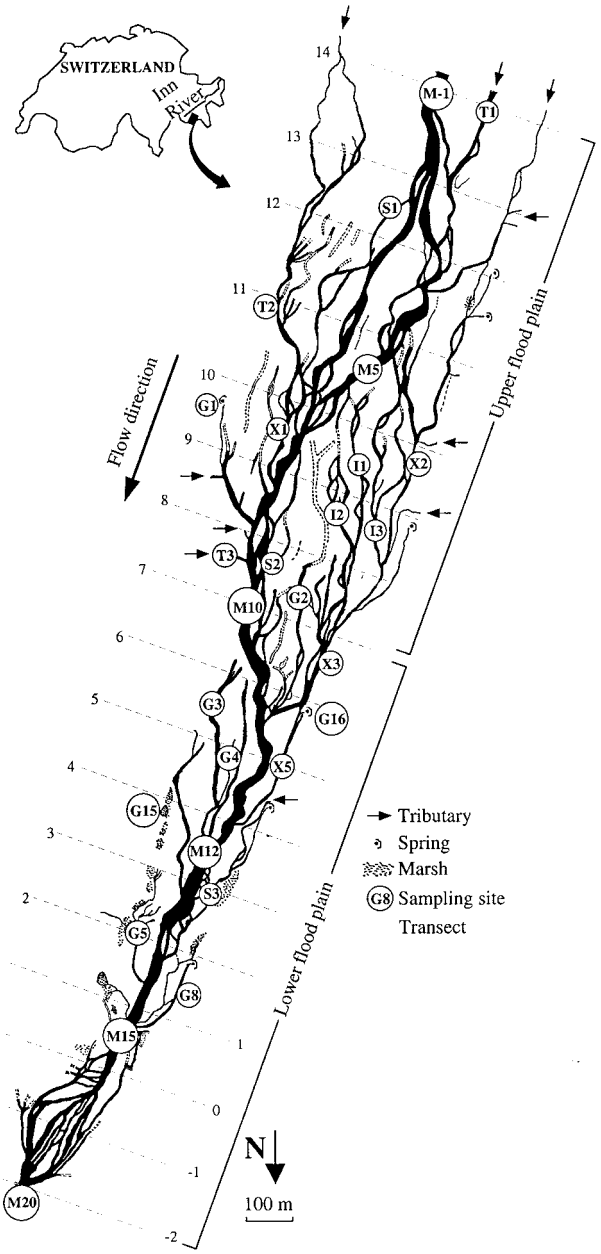

Figure 1. Location and detailed map of the flood plain showing the location of transects and sampling sites. Sampling sites are designated by codes explained in the text.

groundwater (Ward et al. 1999, Malard et al. 1999). In spring (April–June), snowmelt is the main source of water for the entire floodplain, although it circulates via subsurface pathways on the catchment slopes before entering the floodplain. Peak discharge in summer (July–mid September) is associated with the melting of the glaciers. In autumn (mid September–December), seepage of glacial water from the main channel is the main water source for the upper floodplain whereas surface flow in the lower floodplain is sustained by upwelling of deep alluvial and hillslope groundwater. Glacial water and groundwater have contrasting chemical characteristics (Ward et al. 1999; Malard et al. 1999). Melting of the glaciers results in a fast flow of turbid and dilute water (turbidity > 100 NTU; specific conductance <40 μS cm^{-1}) whereas groundwater is clear and enriched in solutes (turbidity < 16 NTU; specific conductance > 60 μS cm^{-1}).

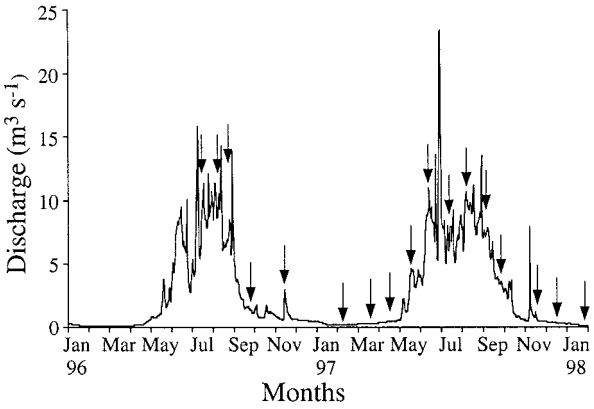

Figure 2. Hydrograph of the Roseg River in 1996 and 1997 (daily discharge). Arrows indicate the sampling dates.

River discharge is continuously recorded by the Swiss Hydrological Geological Survey 7.2 km downstream from the floodplain terminus (Figure 2). Mean annual discharge for the period 1955–1994 was 2.8 m^{3}s^{-1}; mean discharge in 1996 and 1997 was 2.5 and 3.1 m^{3}s^{-1}, respectively. A six-year flood (peak discharge: 35 m^{3}s^{-1}) occurred on 29 June 1997. Although the flood had minimal effects on channel shifting, it increased hydrological connections between the main channel and adjacent channels of the flood plain (e.g., sites I1, I3, X2 and X3 in Figure 1).

Mapping of the channel network

In July 1996, the exact position, depth and wetted width of individual channels, springs, and marshes were measured along 17 transects (150 m–200 m apart) perpendicular to the longitudinal axis of the flood plain (Figure 1). In September 1996, aerial photographs (colour and IR (infrared) images, spatial resolution: 0.1 m) were taken from a helicopter at 500 m above ground level. The field measurements and aerial photographs were combined to produce a digitized map of the floodplain channel network. From

July 1996 to January 1998, subsequent changes in the channel pattern were recorded during 17 field surveys carried out at monthly intervals.

Physico-chemical sampling of surface water

Physico-chemical investigations were carried out following the same time schedule as the channel network mapping. Turbidity (turbidity meter Cosmos, Fa. Züllig, Rheineck, Switzerland) and specific conductance (specific conductance meter WTW LF 323-B/Set; reference temperature 20 °C) were systematically recorded in each channel along the 17 transects within the flood plain. Measurements were completed early in the morning (600–900 hrs) to avoid changes in water chemistry associated with daily discharge fluctuations. In addition, measurements were carried out late in the afternoon on 23 August 1996 during maximum glacier ablation. The number of sample locations for a particular survey varied from 27 to 130 depending on the number of channels carrying water. From July 1996 to January 1998, the total number of measurements was 1367 for turbidity and 1483 for specific conductance.

Sampling of 13 other parameters (see below) was carried out at a number of sites that were distributed across the flood plain and included all channel types (Figure 1). The number of these sampled sites seasonally varied from 9 to 27 according to the number of flowing channels. A total of 319 water samples were analyzed for these additional parameters. Water was collected in 1-L polyethylene bottles, filtered (Whatman GF/F filters; 0.7 μm) within one to four hours, and stored for one to three days at 4 °C prior to analysis.

Physico-chemical analyses of water

A total of 4785 single parameter analyses were performed during the investigation. Calcium and magnesium were analyzed with an Inductively Coupled Plasma-Optical Emission Spectrometer (SPECTRO Analytical Instruments, Kleve, Germany). Bicarbonate determination was made by CO_2 detection (Horiba IR-detector) after samples had been acidified and heated to 860 °C. Ammonium and nitrate were measured with the indophenol-blue method (D.E.V. 1985) and the automated hydrazine reduction method (Downes 1978), respectively. Soluble reactive phosphorous (SRP) was measured with the molybdenum blue method (Vogler 1965). Total dissolved phosphorous (TDP) was determined as SRP after digestion with $K_2S_2O_8$ at 121 °C, and dissolved non-reactive phosphorous (NRP) was calculated as the difference between TDP and SRP. Dissolved organic carbon (DOC) was measured by wet oxidation with subsequent acidification and CO_2 IR-detection (A.P.H.A. 1989). Total suspended solids (TSS) and volatile suspended solids (AFDM) were determined according to A.P.H.A. (1989). Inorganic suspended solids (ISS) were calculated as the difference between TDS and AFDM. Particulate phosphorus (PP) and particulate nitrogen (PN) were quantified as SRP and NO_3-N, respectively, after digestion with $K_2S_2O_8$ at 121 °C. Particulate organic carbon (POC) was determined by combustion at 880 °C and subsequent measurement of the generated CO_2 with a Horiba IR-detector (Uehlinger et al. 1984).

Data analysis

Categorical color maps of the floodplain channels were developed (Map Info Software) to examine changes in the spatial pattern of turbidity and specific conductance (Figures 3 and 4). Values for these 2 parameters were distributed into 8 classes, a geometric series for turbidity (0–2, 2–4, 4–8, 8–16, 16–32, 32–64, 64–128, >128 NTU) and a linear series for specific conductance (15–30, 30–40, 40–50, 50–60, 60–70, 70–80, 80–90, >90 μS cm^{-1}). For the sake of clarity, we preferred to use even classes although turbidity and specific conductance data were not normally distributed. Preliminary tests also indicated that the number of classes (8 *versus* 17 even classes) had little effect on the Shannon-Wiener diversity index used to quantify riverscape heterogeneity (see below). A different color pattern was plotted for each length of channel corresponding to the 8 classes defined above. For the purpose of mapping, the entire channel segment was placed into a single color class if that channel segment transversed only one measuring transect. In cases where a channel segment crossed multiple measuring transects, a color class was associated with the length of channel extending equidistant between two consecutive transects (typically 75 m upstream or downstream of a particular transect).

From a landscape perspective, spatial heterogeneity in river-floodplain systems can be visualized as a shifting mosaic (*sensu* Gustafson 1998). The aquatic mosaic or riverscape has 3 components: extent, composition (non-spatial), and configuration (spatial). Because all these components of heterogeneity could influence biodiversity and ecosystem processes (Stan-

ley et al. 1997; Cooper et al. 1997), we attempted to analyze each of them. For example, in the Val Roseg flood plain, the proportion of channel length carrying water of different turbidity influences light availability and, thereby, determines the development of benthic algae and primary production (Uehlinger et al. 1998). Spatial patterns of organic matter processing may also reflect landscape-level attributes (Robinson et al. 1998).

To characterize variation in the extent and morphology of the floodplain channel network, we measured the total channel length (T in km) and computed the index of surface connectivity (SC) (Table 1). T expresses the expansion/contraction of the channel network and SC indicates the proportion of the total channel length that has an upstream surface connection with the main channel.

Temporal changes in the spatial heterogeneity of turbidity and specific conductance were analyzed using indices of landscape pattern (Romme 1982; O'Neill et al. 1988; Hoover and Parker 1991; Gustafson 1998) (Table 1). Patch-based indices evaluate the spatial configuration of the mosaic whereas richness and evenness refer to its composition. We defined a patch as a continuous length of channel belonging to a particular turbidity or specific conductance class. Thus, on the categorical maps (Figures 3 and 4), a patch corresponds to a set of interconnected channels having the same color. Then, we determined the total number of patches in the flood plain (N), the average length of a patch (L in km) and its coefficient of variation (CV) as a measure of variability in length among patches. Richness (R), evenness (E) and contrast (C) were expressed as relative indices, i.e., as a percent of the maximum possible value (Table 1). Richness was a sum of the number of turbidity classes and specific conductance classes represented in the flood plain. Evenness measured the proportions of channel length representation among classes and was determined using the modified Simpson's index (Pielou 1975; Romme 1982). The sum of the dissimilarity values for all surface hydrological connections between patches measured the collective degree of contrast (C) among adjacent patches in the flood plain (Romme 1982; Hoover and Parker 1991). The dissimilarity value for a particular connection between 2 patches was allowed to vary linearly from a minimum of 1/7, when the patches belonged to 2 consecutive classes, to a maximum of 7/7, when patches belonged to the most distant classes. Riverscape heterogeneity (RH) was measured in two different ways. First, richness, evenness, and contrast were averaged (RH1). Second, the Shannon–Wiener diversity index (RH2; Pielou 1975) was computed using the proportion of total channel length covered by a class as the measure of its abundance.

We examined the relationships between riverscape heterogeneity in turbidity and specific conductance and river discharge, water source, expansion/contraction of the channel network, and hydrological connectivity. This was achieved by plotting RH1 versus discharge recorded at the time of sampling (i.e., 600-900 hrs), specific conductance measured at site M20 (Figure 1), total channel length (T), and surface hydrological connectivity (SC). Specific conductance at the floodplain outlet (site M20) was used as an indicator of the relative contributions of the glaciers and groundwater reservoirs to the flow rate of water in the flood plain (Malard et al. 1999; Ward et al. 1999).

We determined whether riverscape heterogeneity calculated from turbidity and specific conductance data would reflect overall chemical heterogeneity of surface water. To this end, a temporal series of floodplain maps showing physico-chemical heterogeneity of surface water was generated as follow. The initial physico-chemical data table (a maximum of 27 sites, 15 dates, and 15 physico-chemical variables) was analyzed by means of a within-dates principal component analysis (PCA) (Dolédec and Chessel 1987, 1991). This type of multivariate analysis provides a set of spatial typologies of sampling sites that can be compared between each other. Briefly explained, the within-dates PCA of the initial physico-chemical data table is simply the PCA of the residuals per date (i.e., the average per date is removed from the original data). Diagonalization of the transformed table generates new axes (i.e., eigenvectors or principal components) and the factorial scores of variables and sampling sites for each axis. Eigenvalues indicate the amount of variance in the data set explained by each axis. Factorial scores of variables, which correspond to correlation coefficients between the physico-chemical variables and the axes, are plotted on a correlation diagram. Absolute contributions define the variables most responsible for the appearance of an axis whereas the relative contributions describe how a variable is related to the different axes. Because factorial scores of sites are new synthetic variables generated by the analysis, they can be used for mapping (Dolédec and Chessel 1991). For each sampling date, factorial scores of sampling sites along the first axis of the PCA were plotted directly on

Table 1. Indices used to characterize the channel network and spatial heterogeneity in turbidity and specific conductance. Logarithm base 2 was used to compute evenness (E) and Shannon–Wiener diversity index (RH2).

1. Total channel length (T in km)
Sum of the lengths of all channels with surface water flow
2. Surface hydrological connectivity (SC)
$\mathrm{Sc} = \frac{Tc}{T}$, where Tc = length of channels having an upstream connection with the mian channel
3. Total number of patches (N)
A patch is defined as a continous lenght of channel belonging to a
particular turbidity or specific conductance class.
4. The average length of a patch (L in km)
$L = \frac{\sum_{i=1}^{N} 1_i}{N}$, where l_i = length of patch i
5. Coefficient of variation of the average length of a patch (CV)
$\mathrm{CV} = \frac{\sigma}{L} \times 100$, where σ = standard deviation of the average length of a patch
6. Relative richness (R)
$R = \frac{r}{8}$, were r = number of different turbidity or specific conductance classes present. Maximum possible number is 8
7. Relative evenness (E)
$E = \frac{-\log \sum_{i=1}^{r} p_i^2}{\log r}$, where p_i = proportion of totoal channel length occupied by ith turbidity or specific conductance class.
8. Relative contrast (C)
$C = \frac{\sum_{i=1}^{B} d_i}{B}$, where B = number of boundaries between adjacent patches in the flood plain
d_i = dissimilatory value for the ith boundary between 2 adjacent patches
9. Diversity (H)
$\mathrm{RH1} = \frac{R+E+C}{3}$
$\mathrm{RH2} = -\sum_{i=1}^{r} p_i \log p_i$

a floodplain map using squares and circles, the surface area of which is proportional to the absolute values of the factorial scores. White squares and grey circles were used to indicate positive and negative factorial scores, respectively. These maps provide an easy way to detect seasonal changes in spatial heterogeneity by comparing differences among dates between factorial scores of sites. The multivariate analysis and graphical displays were done using ADE software (Chessel and Dolédec 1996) and GraphMu software (Thioulouse 1989).

Results

Morphology of the floodplain channel network

The channel network experienced a marked seasonal cycle of expansion and contraction (Figures 3 and 4). The total channel length (T) varied from 5.9 km on 27 January 1998 to 21.4 km on 2 September 1997 (Figure 5). Reduction in T was much more pronounced in the upper flood plain ($\Delta T = -92\%$) than in the lower flood plain ($\Delta T = -36\%$). T increased with discharge (Q), but the relation was logarithmic ($T = 3.8 \ln Q + 13.9$; $n = 17$; $r^2 = 0.93$). Indeed, the length of the stream network was much more sensitive to changes in discharge at Q values < 1.5 m^3 s^{-1}.

Surface hydrological connectivity (SC) was distinctly higher in summer than in winter (Figure 5). The proportion of the total channel length having an upstream connection with the main channel ranged from 5.1% on 4 February 1997 to 44.8% on 2 August 1997. For T > 15 km, SC increased linearly with the total channel length ($\mathrm{SC} = 0.054T - 0.74$; $n = 11$; $r^2 = 0.85$; $p < 0.01$). However, for $T < 15$ km, channel expansion and contraction occurred without appreciable change in surface hydrological connectivity (i.e., SC ca. 5%). For a given discharge value, SC measured in summer (Q ca. 6 m^3 s^{-1}) was higher in 1997 (SC= 31%) than in 1996 (SC = 44%).

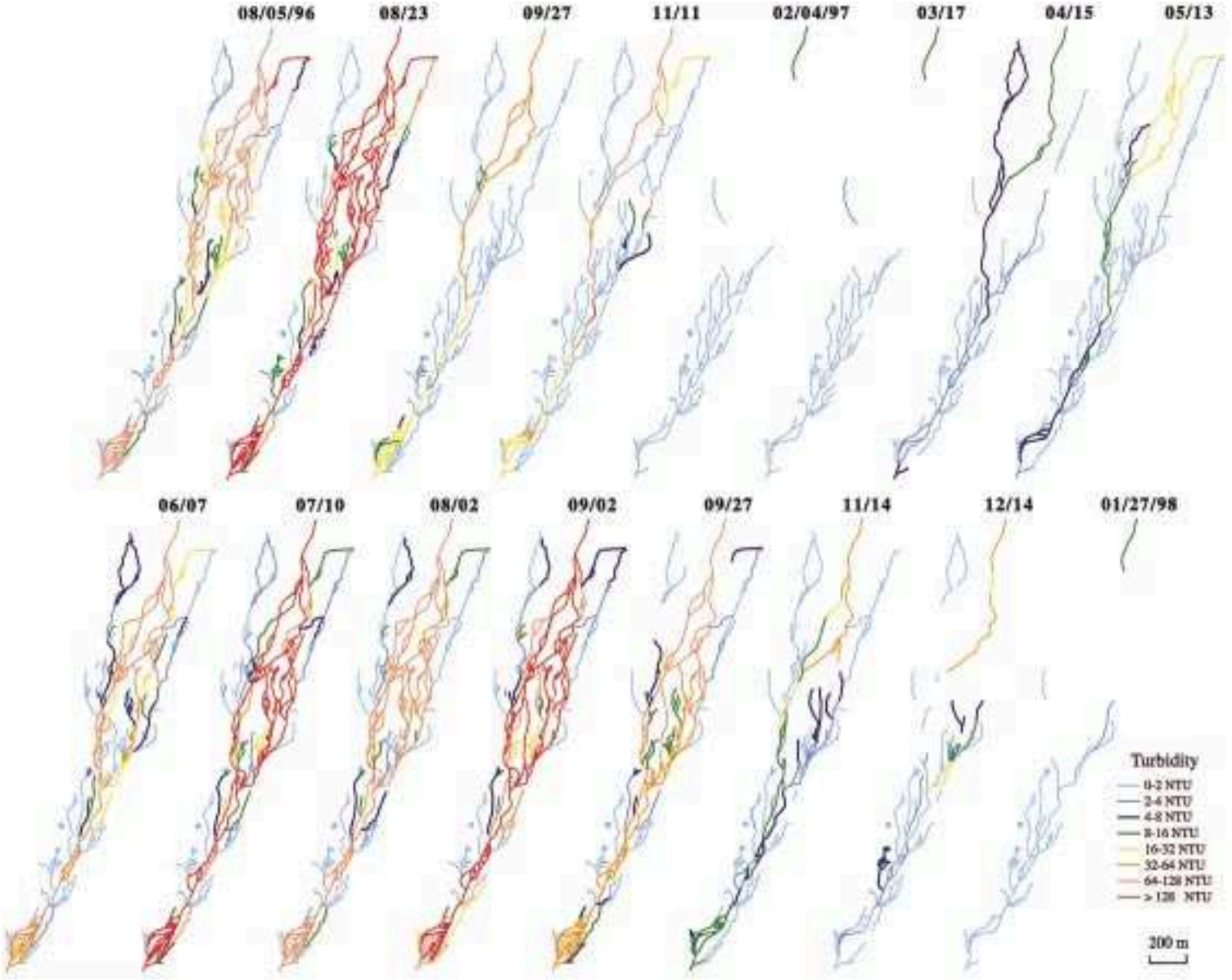

Figure 3. Map showing the distribution of turbidity (August 1996–January 1998) in the Roseg River flood plain. Dates are month/day/year.

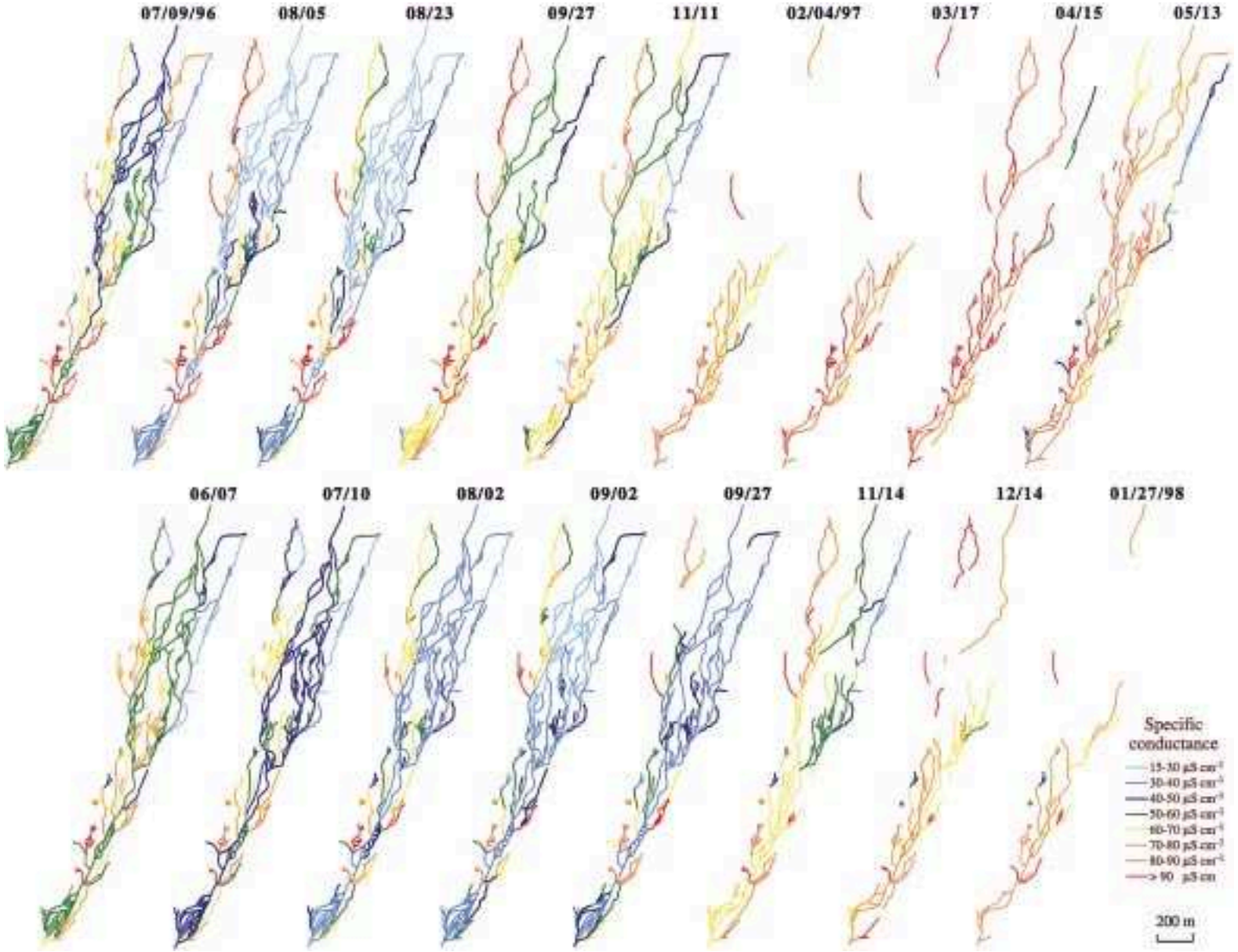

Figure 4. Map showing the distribution of specific conductance (July 1996–January 1998) in the Roseg river flood plain. Dates are month/day/year.

Spatial heterogeneity of turbidity and specific conductance

Categorical color maps of turbidity and specific conductance provided the clearest representation of temporal changes in the values and spatial pattern of these 2 parameters (Figures 3 and 4). Turbidity decreased and specific conductance increased in most floodplain channels during winter. Overall, the flood plain shifted from a complex mosaic in summer to a rather monotonous landscape in winter, when turbidity and specific conductance were rather uniform across the flood plain. The maps portray the lateral and longitudinal development in summer of an expanding corridor that transports water of high turbidity and low specific conductance. The maps also allow the detection of longitudinal and lateral gradients within the flood plain during particular periods. For example, turbidity decreased and specific conductance increased in the lower flood plain during the contraction phase (September, November, and December). A similar gradient was observed in summer along the lateral dimension in groundwater channels located in the lower flood plain (e.g., sites G4, G3, and G5 on 5 August 1996).

Temporal changes in the values of indices quantify spatial heterogeneity on the categorical maps (Figure 6). With the exception of average patch length (L) and evenness (E), all indices exhibited distinct seasonal trends for both turbidity and specific conductance. The total number of patches (N) ranged from 2 to 62 for turbidity and from 13 to 51 for specific conductance. For both parameters, N was positively correlated with the total channel length (Turbidity: $N = 2.8T - 11.8; n = 16; r^2 = 0.85; p < 0.01$; specific conductance: $N = 2T + 3.35; n = 17; r^2 = 0.88; p < 0.01$). Because N increased linearly with T, one-way analysis of variance followed by Tukey's multiple comparison test did not reveal any difference between dates in the average length of a patch (data for turbidity in February, March 1997, and January 1998 were excluded from the analysis). However, the coefficient of variation (CV) increased markedly in summer indicating stronger differences between lengths of individual patches. For specific conductance, the difference in length between the shortest and the longest patches was 1 km on 15 April 1997 and 12.7 km on 2 August 1997. Higher variability in length among patches in summer was mainly due to the presence of a few very long patches (e.g., up to 12.8 km in length for turbidity on 23 August 1996) within the floodplain corridor. The appearance of additional patches outside the corridor compensated for the formation of these long patches because N did not decrease nor reach a plateau as T increased (Figures 3 and 4).

Richness (R) was markedly lower during winter. Out of the 8 possible classes, only 2 and 4 were represented for turbidity (4 February 1997) and specific conductance (17 March 1997), respectively. Evenness (E) showed a distinct temporal pattern only for turbidity (Figure 6). The lowest E for turbidity was observed in winter when almost all water bodies located in the lower flood plain had turbidity values below 2 NTU (Figure 3). Evenness for specific conductance was at minimum on 2 August and 27 September 1997, when 60% of the total channel length belonged to only one class (i.e., 30–40 μS cm^{-1}). Values of E were markedly higher in summer 1996 than in summer 1997 for specific conductance but this between-year difference was not observed for turbidity. Floodplain contrast (C) was low in winter and high during the ablation period, the seasonal variability being more pronounced for turbidity. Due to the lack of connections between patches in February and March 1997, C was equal to zero for turbidity. Higher C in summer was mainly attributable to an increase in the dissimilarity values between the floodplain corridor and groundwater-fed channels (i.e., groundwater channels or tributaries). The two indices of riverscape heterogeneity, i.e., the average of richness, evenness, and contrast (RH1) and the Shannon–Wiener index (RH2), showed similar temporal patterns. Riverscape heterogeneity was highest in summer and fell to a low level in winter, this trend being more pronounced for turbidity. Decreases in E caused by the development of the floodplain corridor did not result in a marked reduction of either RH during the summer. For specific conductance, RH was higher in summer 1996 (RH1=0.7) than in summer 1997 (RH1=0.6).

RH versus Q, water source, T, and SC

Riverscape heterogeneity for turbidity and specific conductance (RH1) was plotted against discharge (Q), specific conductance measured at site M20, total channel length (T), and surface hydrological connectivity (SC) (Figure 7). For all these variables, we used a second order polynomial function to describe their relationships with diversity. The points roughly follow the increasing limb of a polynomial function for discharge, total length and surface hydrological connectivity and the decreasing limb of a polynomial function for specific conductance measured at site

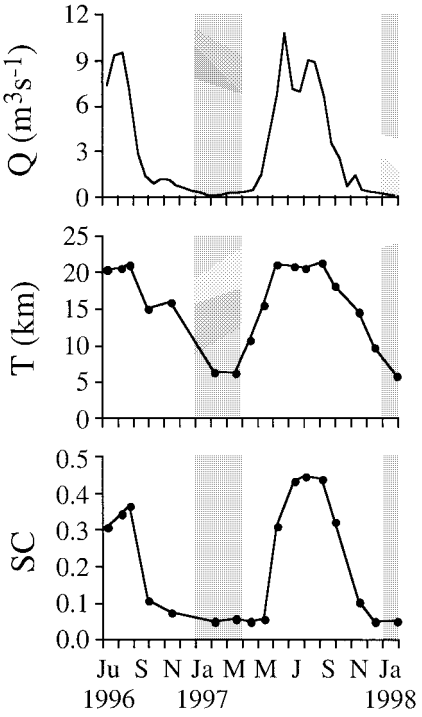

Figure 5. Temporal changes in river discharge (Q; biweekly average), total channel length (T) and surface hydrological connectivity (SC). The shaded area indicates winter.

M20. The proportion of variance in RH accounted for by the regression model (r^2 in Figure 7) ranged from 0.37 to 0.90 ($r^2 > 0.5$ in 6 cases out of 8). However, the relation between RH and SC must be considered with caution because points are grouped into two clusters. For a particular variable, r^2 was always higher for turbidity than for specific conductance. Considering only the sampling dates prior to the flood in June ($n = 9$ for turbidity; $n = 10$ for specific conductance), we reiterated the same polynomial regression model. This procedure had no effect on the goodness of fit of the model for turbidity but it resulted in an increase in r^2 for specific conductance: from 0.37 to 0.49 for Q, 0.63 to 0.89 for specific conductance measured at site M20, 0.59 to 0.73 for T, and 0.47 to 0.56 for SC.

Spatial heterogeneity of other physico-chemical parameters

For each sampling date, the average concentrations (± standard deviation) of 15 physico-chemical parameters measured at multiple sites are indicated in Table 2. All parameters, except POC, PN, NRP, SRP, and DOC showed a distinct seasonal pattern. Summer concentrations of ISS, AFDM, NH_4^+, PP, and turbidity

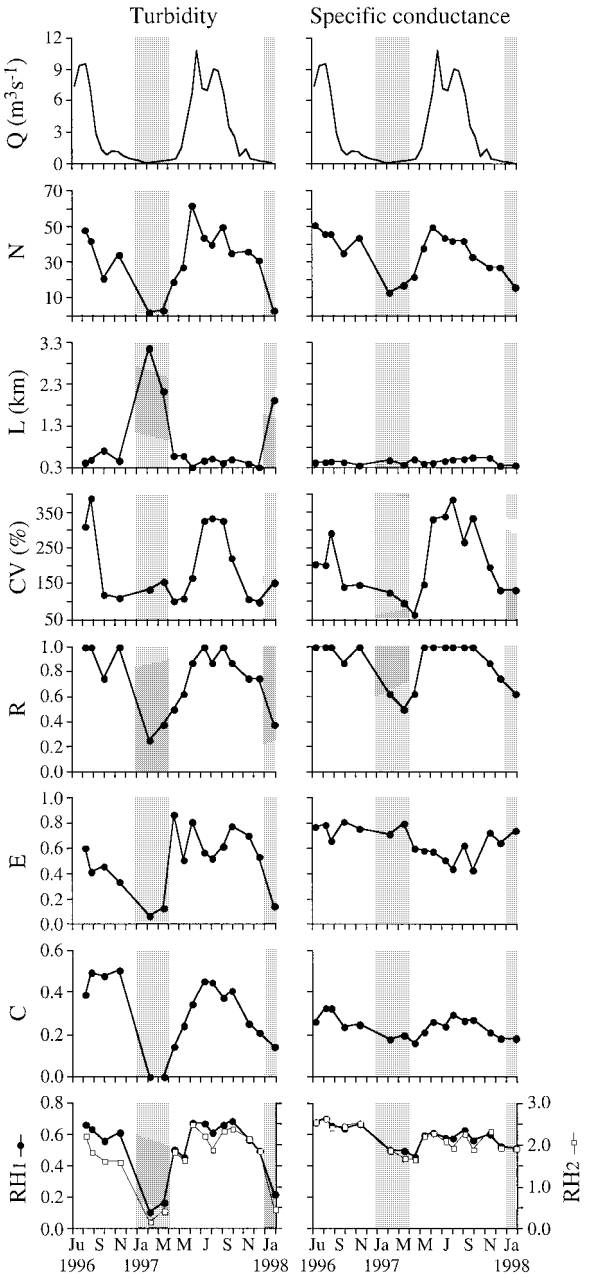

Figure 6. Temporal changes in river discharge (Q; biweekly average), the number of patches (N), the average length of patches (L), its coefficient of variation (CV), the relative richness (R), the evenness (E), the contrast (C) and the riverscape heterogeneity (RH1 and RH2) as measured for turbidity (left panel) and specific conductance (right panel). The shaded area indicates winter.

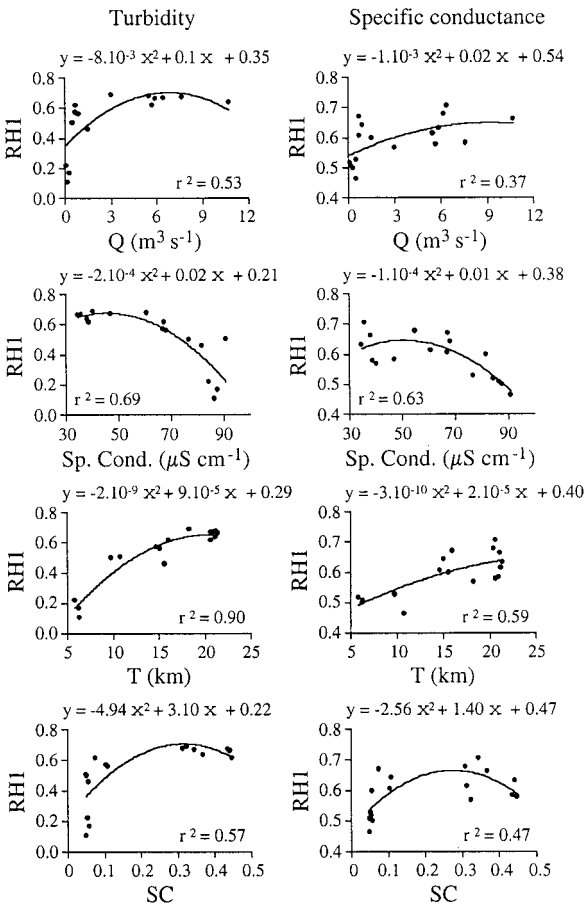

Figure 7. Relation between riverscape heterogeneity (RH1) as measured for turbidity (left panel) and specific conductance (right panel) and discharge (Q), specific conductance at the floodplain outlet (Sp. Cond.), total channel length (T), and surface hydrological connectivity (SC). Specific conductance at the floodplain outlet is used as an estimate of the relative contributions of glacial water and groundwater to the flow rate of water in the flood plain.

were significantly higher than the winter concentrations ($p < 0.01$; ANOVA). The reverse was observed for Ca^{++}, Mg^{++}, HCO_3^-, and specific conductance. Standard deviations for all these parameters increased during the summer. NO_3^- also fluctuated seasonally but concentrations peaked in spring (April, May).

Sixty-four percent of the variance in the initial physico-chemical data set was attributed to the within-date PCA (removal of the time effect), of which 44% and 14% were explained by the first and second axes of the analysis, respectively. Two groups of physico-chemical variables accounted for 99.6% of the appearance of the first axis (see absolute contributions in Table 3): turbidity, ISS, AFDM, PP, POC, NH_4^+, and PN in the negative region of the axis, and

Table 2. Means (± standard deviation) of 15 physico-chemical variables measured in surface water of the Roseg River flood plain during 15 sampling dates. For each date, the number of sampling sites is indicated in parentheses.

	Sampling dates														
	08/05 1996 (23)	09/27 (20)	11/11 (20)	02/04 1997 (9)	03/17 (12)	04/15 (17)	05/13 (24)	06/07 (27)	07/10 (27)	08/02 (27)	09/02 (27)	09/27 (26)	11/14 (24)	12/14 (22)	01/27 1998 (14)
ISS (mg L^{-1})	23.4 ± 23.6	6.4 ± 7.6	12.3 ± 13.5	0.9 ± 0.8	2.0 ± 2.4	1.9 ± 2.7	3.2 ± 3.1	13.2 ± 16.0	63.8 ± 62.6	27.9 ± 24.6	27.0 ± 24.1	16.6 ± 14.0	5.4 ± 4.8	2.1 ± 3.5	2.0 ± 2.9
AFDM (mg L^{-1})	2.1 ± 0.9	2.0 ± 1.0	1.8 ± 0.7	1.3 ± 0.3	1.4 ± 0.1	1.7 ± 0.2	1.6 ± 0.2	1.7 ± 0.4	3.7 ± 2.1	2.9 ± 1.2	2.7 ± 0.9	1.7 ± 0.5	1.6 ± 0.4	1.5 ± 0.4	1.5 ± 0.4
POC (mg L^{-1})	0.18 ± 0.08	0.13 ± 0.06	0.19 ± 0.07	0.16 ± 0.07	0.09 ± 0.05	0.13 ± 0.07	0.12 ± 0.07	0.17 ± 0.05	0.29 ± 0.16	0.21 ± 0.09	0.19 ± 0.06	0.19 ± 0.05	0.16 ± 0.04	0.15 ± 0.07	0.20 ± 0.09
NH_4^+-N (μg L^{-1})	5 ± 5	3 ± 3	4 ± 2	3 ± 1	2 ± 2	3 ± 2	1 ± 1	1 ± 1	6 ± 5	7 ± 7	9 ± 7	4 ± 2	2 ± 2	2 ± 2	3 ± 2
NO_3^--N (μg L^{-1})	241 ± 77	241 ± 41	230 ± 60	261 ± 32	352 ± 42	409 ± 51	394 ± 82	357 ± 106	232 ± 92	227 ± 60	178 ± 50	164 ± 45	212 ± 42	233 ± 35	219 ± 41
PN (μg L^{-1})	16 ± 9	11 ± 7	20 ± 10	14 ± 5	9 ± 7	12 ± 6	14 ± 8	12 ± 4	15 ± 7	13 ± 7	14 ± 6	10 ± 5	8 ± 4	6 ± 5	13 ± 6
PP (μg L^{-1})	22 ± 22	7 ± 7	14 ± 16	1 ± 1	3 ± 7	3 ± 2	6 ± 9	13 ± 16	60 ± 58	24 ± 23	22 ± 19	14 ± 10	10 ± 8	3 ± 4	3 ± 3
NRP (μg L^{-1})	1 ± 3	1 ± 1	1 ± 1	1 ± 1	1 ± 1	3 ± 1	3 ± 1	1 ± 1	5 ± 1	2 ± 1	3 ± 2	1 ± 1	3 ± 1	1 ± 1	1 ± 1
SRP (μg L^{-1})	3 ± 2	1 ± 1	1 ± 1	1 ± 1	1 ± 0	2 ± 1	1 ± 2	1 ± 1	3 ± 1	2 ± 1	1 ± 1	1 ± 0	1 ± 1	1 ± 1	1 ± 1
DOC (mg L^{-1})	0.5 ± 0.2	0.7 ± 0.3	0.8 ± 0.7	0.8 ± 0.2	0.4 ± 0.1	0.5 ± 0.1	0.5 ± 0.4	0.4 ± 0.2	0.5 ± 0.3	0.2 ± 0.1	0.2 ± 0.2	0.5 ± 0.2	0.3 ± 0.1	0.5 ± 0.2	0.3 ± 0.1
Ca^{++} (mg L^{-1})	8.5 ± 4.4	11.8 ± 2.7	12.5 ± 2.3	16.5 ± 2.7	16.2 ± 2.3	16.7 ± 2.9	14.5 ± 2.1	12.0 ± 2.9	8.8 ± 2.4	9.3 ± 3.6	8.9 ± 3.9	9.6 ± 4.3	12.4 ± 2.2	14.2 ± 2.2	14.4 ± 2.9
Mg^{++} (mg L^{-1})	0.8 ± 0.4	0.9 ± 0.4	0.9 ± 0.3	1.4 ± 0.3	1.2 ± 0.3	1.3 ± 0.3	1.0 ± 0.2	0.9 ± 0.3	0.7 ± 0.3	0.7 ± 0.4	0.7 ± 0.4	0.8 ± 0.4	0.9 ± 0.3	1.1 ± 0.4	1.3 ± 0.4
HCO_3^- (mg L^{-1})	23.9 ± 12.0	33.5 ± 6.7	29.1 ± 6.4	39.7 ± 3.8	39.2 ± 4.5	39.9 ± 4.8	37.3 ± 4.2	30.0 ± 7.1	27.4 ± 8.1	25.5 ± 10.9	24.6 ± 10.2	25.0 ± 11.0	30.5 ± 5.7	32.4 ± 4.8	35.4 ± 6.4
Cond. (μS cm^{-1})	46 ± 21	69 ± 14	66 ± 13	81 ± 17	89 ± 14	91 ± 13	78 ± 10	63 ± 14	52 ± 13	49 ± 19	46 ± 20	49 ± 22	68 ± 14	74 ± 11	82 ± 18
Turb. (FTU)	39 ± 39	14 ± 22	22 ± 28	1 ± 0.4	2 ± 4	2 ± 2	5 ± 7	23 ± 28	112 ± 108	50 ± 46	58 ± 51	36 ± 33	9 ± 12	5 ± 9	2 ± 4

HCO_3^-, Ca^{++}, specific conductance, and Mg^{++} in the positive region (Figure 8A). Most of these variables had more than half of their variability related to the first axis (see relative contributions in Table 3). Within the 2 clusters, all variables were significantly correlated ($p < 0.01$, $n = 319$), the Pearson's correlation coefficient (r) ranging from 0.37 to 0.98 and from 0.78 to 0.97 for the negative and positive groups, respectively. Only 4 variables out of 15, i.e., NO_3^-, NRP, SRP and DOC were poorly related to axis 1 (relative contributions <1.5% in Table 3).

Factorial scores of sampling sites along axis 1 of the PCA are plotted on a series of floodplain maps in Figure 8B. The seasonal shift in the spatial pattern of heterogeneity provided by these maps is similar to that obtained with turbidity and specific conductance. White squares of similar size indicate that water chemistry was spatially homogeneous in winter. Specific conductance and concentrations of major ions were high, whereas turbidity, concentrations of particulate parameters, and ammonium were low in all water bodies of the flood plain. Physico-chemical differences between sites increased in spring and were maximum in summer. During summer, sampling sites within the corridor of high turbidity/low specific conductance water had similar negative scores along the first axis. They carried turbid water, which had high concentrations of particulate parameters and ammonium but low specific conductance and concentrations of major ions. Surface water outside the corridor had the opposite physico-chemical characteristics, and there were marked differences among sites. For example, PP concentrations in channels located outside the corridor varied from 1 μg L^{-1} at site Q5 to 23 μg L^{-1} at site T3 on 10 July 1997.

Table 3. Absolute and relative contributions of variables to axis 1 from within-date principal component analysis.

	Absolute contribution	Relative contribution
ISS	11.8	79.0
AFDM	11.5	76.9
POC	8.7	49.9
NH_4^+	8.2	47.7
NO_3^-	0.0	0.1
PN	5.6	30.0
PP	11.3	73.2
NRP	0.0	0.1
SRP	0.0	0.2
DOC	0.3	1.5
Ca^{++}	7.3	54.9
Mg^{++}	6.1	36.1
HCO_3^-	10.1	61.6
Cond.	7.0	55.1
Turb.	12.0	79.7

Discussion

Expansion/contraction of the floodplain channel network

Aquatic habitats of river-floodplain systems undergo major changes in size, but the spatial pattern of expansion and contraction varies between systems (de Vries 1995; Stanley et al. 1997). In the Val Roseg, the first phase of expansion (from March to May 1997) was linked to the recharge of hillslope and alluvial aquifers by snow-melt water (Malard et al. 1999). This recharge mainly sustained the flow of surface water in groundwater-fed tributaries and groundwater channels within the flood plain (Figure 3). Therefore, the increase in channel length (from 6 to 15 km as Q increased from 0.3 to 1.5 m^3 s^{-1}) occurred without substantial changes in surface hydrological connectivity (i.e., SC∼5%). In a similar way, SC did not vary during the second phase of contraction (from December to January 1998), that was mainly due to a progressive decline of the water table of the floodplain aquifer. Tockner et al. (1999) defined 3 major phases of hydrological connectivity between the Danube River and its flood plain: disconnection, seepage inflow, and upstream surface connection. During the second phase, the water levels of floodplain water bodies fluctuated in response to seepage inflow through porous aquifers. From May to August 1997, overflow of main channel water in the Val Roseg flood plain caused a further expansion of the channel network (from 15 to 21.4 km as Q increased from 1.5 to 6 m^3 s^{-1}) and a marked increase in surface hydrological connectivity (from 5 to 44.8%). However, this second phase of expansion did not result in an increase in the proportion of lentic habitats as it is often the case in flood plains traversed by a moving littoral (Roux 1982; Junk et al. 1989). With the exception of marshes on the floodplain terraces, the aquatic habitats in the Val Roseg consist only of lotic water bodies.

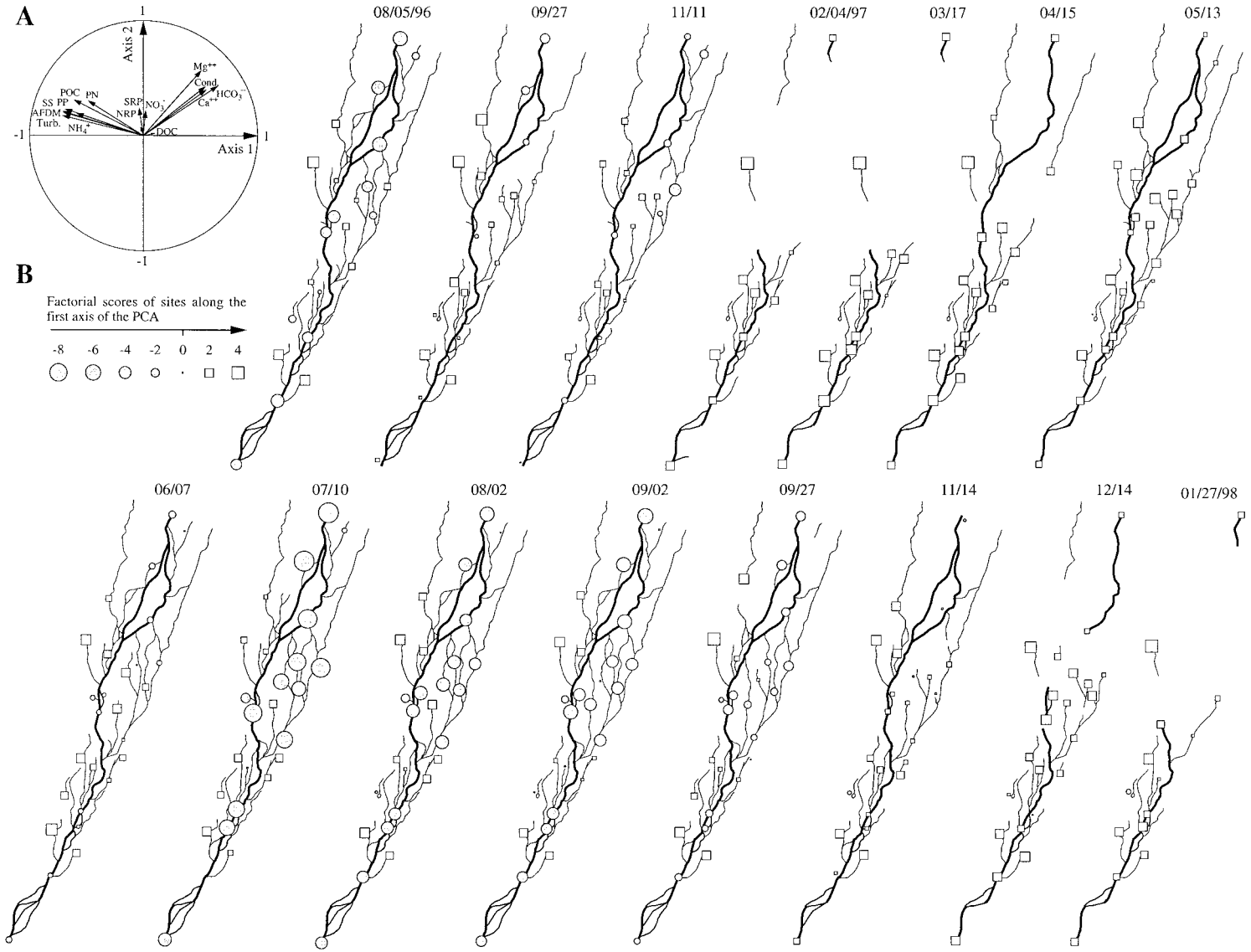

Figure 8. Graphical presentation of the within-date principal component analysis (PCA). (A) Correlation diagram for the physico-chemical variables. (B) Plot of factorial scores of the samples (axis 1 of the within-date principal component analysis) on a floodplain map for each date. The surface areas of circles and squares are proportional to the sample scores along axis 1. Grey circles and white squares indicate negative and positive scores, respectively.

Hydrological causes of seasonality in riverscape heterogeneity

The physico-chemical heterogeneity of floodplain water is a function of the sources and flow paths of water, autogenic processes operating in different surface water bodies (e.g., biological uptake and release, sedimentation and resuspension of particles) and hydrological connectivity (Juget et al. 1976; Hamilton and Lewis 1987; Forsberg et al. 1988; Van den Brink et al. 1993; Heiler et al. 1995; Knowlton and Jones 1997). Two different aspects of hydrological connectivity must be considered. The first one refers to the linkages between the hydrological reservoirs of the catchment and the river-floodplain systems (Dole 1983, Turner and Macpherson 1990; Bencala 1993; Burt and Haycock 1996). Several hydrological reservoirs, including the glaciers, the snow pack, and groundwaters (hillslope and alluvial groundwaters) contributed to surface flow in the Val Roseg, but their hydrological connectivity with the flood plain differed markedly (Malard et al. 1999; Ward et al. 1999). Groundwater inflows occur at multiple points via surface (e.g., groundwater-fed tributaries) or subsurface flow paths (e.g., diffuse emergence within the flood plain). In contrast, glacial water mainly enters the flood plain at single location via a surface flow path (site M-1 in Figure 1). Thus, its effect on the chemistry of floodplain water depends on the second aspect of hydrological connectivity, i.e., the exchange of water between the different surface water bodies (Amoros and Roux 1988; Heiler et al. 1995; Ward and Stanford 1995).

Decrease in riverscape heterogeneity during periods of upstream disconnection with the main channel (i.e., autumn and winter) was due to the increasing dominance of ground water. Independently of the strength of hydrological linkages between surface water bodies, multiple emergences of ground water in the flood plain had a strong homogenizing effect on turbidity and specific conductance. This effect was even more pronounced for turbidity because groundwater sources of different specific conductance had similar turbidity (< 2 NTU). The disappearance of most turbidity classes in winter resulted in a marked reduction in the number of patches and a concomitant increase in the average length of a patch. Seepage of main channel water in the upper flood plain *versus* upwelling of deep ground water (hillslope and alluvial groundwater) in the lower flood plain caused longitudinal changes in specific conductance in autumn. However, this spatial gradient progressively disappeared as the latter source of water became dominant in winter. Spatial heterogeneity in specific conductance in floodplain-river systems during low water is likely to reflect the variety and relative importance of local inputs of water. Juget et al. (1976) reported substantial differences in specific conductance (i.e., 250–600 μS cm^{-1}) between floodplain water bodies of the Rhône River during low-water periods. Differences in particle sedimentation, sediment resuspension and phytoplankton development among floodplain water bodies may result in spatial variation in turbidity during hydrologic isolation from the main channel (Hamilton and Lewis 1987; Heiler et al. 1995; Junk 1997; Knowlton and Jones 1997). However, none of these processes was important in the Val Roseg flood plain, mainly because of the absence of lentic water bodies.

Increase in riverscape heterogeneity for turbidity and specific conductance in spring and summer is attributed to the diversification of water sources (i.e., snow pack, ice, and ground water) and flow paths (i.e., surface, shallow and deep subsurface pathways). As water level increased from snow melt (June) and ice melt (July and August), several channels became connected at their upstream ends with the main channel. This braided corridor which showed little spatial variation in turbidity and specific conductance progressively expanded across the flood plain. The development of this corridor led to greater differences in length between patches and to a reduction in evenness. However, the reduction in evenness associated with the flood pulse was too low to induce a substantial decrease in riverscape heterogeneity during the summer. Similarly, patchiness, defined as the number of patches (N) divided by the total channel length (T), was not markedly reduced during flooding. N might have reached a plateau or even decreased with T if the flood pulse had resulted in the development of a limited number of very long patches. In contrast, the number of patches was shown to increase linearly with T. A decline in the spatial heterogeneity of specific conductance is expected during seasonal peak discharge in river-floodplain systems where all water bodies receive water from the main channel. Peak discharge in a fully connected river-floodplain system also may result in greater spatial homogeneity for turbidity as long as variations in velocity among connected surface water bodies do not induce strong differences in settling rates. In the Val Roseg flood plain, surface hydrological connectivity for the highest discharge considered during the investigation period was probably too low

(SC=44.8%) to induce a substantial decline in spatial heterogeneity. Moreover, increasing homogeneity due to surface connection within the corridor was compensated by increasing heterogeneity due to seepage inflow outside the corridor. Indeed, whereas turbidity and specific conductance of glacial water showed little variation within the braided corridor, bank infiltration and resurfacing of glacial water influenced the physico-chemical characteristics of nearby groundwater channels. For example, groundwater channel G3 contained only 1 patch in April 1997 but 4 patches belonging to 4 specific conductance classes in July 1997 (Figure 4).

Riverscape heterogeneity as discussed above referred to the complexity and variability of turbidity and specific conductance in time and space. However, the physico-chemical attributes of floodplain water integrate a number of biotic and abiotic factors, including biological uptake of nutrients, release and adsorption of solutes by the sediment, mass transport and water balance. In the Val Roseg flood plain, the graphical interpretation of the within-dates PCA showed that the spatial heterogeneity of most parameters was closely related to that observed for specific conductance and turbidity (Figure 8). This result strongly suggests that the relative contribution over space and time of different water sources is the main factor that determines the shifting physico-chemical mosaic. It also implies that turbidity and specific conductance can be used as simple indicators for measuring temporal changes in overall chemical heterogeneity. Unlike the observations made in other river-floodplain systems (Hamilton and Lewis 1987; Forsberg et al. 1988; Bonetto et al. 1994; Heiler et al. 1995; Knowlton and Jones 1997; Tockner et al. 1999), autogenic processes do not seem to play an important role in this glacial flood plain. Of the 4 parameters which did not correspond to the pattern of heterogeneity exhibited by specific conductance or turbidity, NRP, SRP, and DOC always had low concentrations (see Table 2). In a previous study, Tockner et al. (1997) did not find any significant differences in SRP between channel types and reported important spatial variations in DOC (i.e., 0.1–3.4 mg L^{-1}) only during heavy rainfall events that caused leaching of soils on the floodplain terraces. Seasonality in NO_3^- concentrations did not match the pulsing of discharge. As in many other mountain areas (Charles 1991), the spring peak of NO_3^- concentrations strongly suggests that snowpack is the main source of NO_3^- in the Val Roseg. Despite this strong seasonality concentrations never showed a well-defined spatial pattern.

Examining the effects of erosive floods and movements of the glaciers on riverscape heterogeneity

The relationship between riverscape heterogeneity and discharge, as expressed in Figure 7 for turbidity and specific conductance, was established for a given morphology of the channel network. However, any geomorphological modification would affect these relations by changing the degree of hydrological connectivity between floodplain water bodies for a given discharge. As in many other glacial systems (Maizels 1983; Gregory 1987; Milner and Petts 1994), the channel system of the Val Roseg flood plain is unstable and responds to changes in discharge and sediment delivery caused by unpredictable erosive floods and the movements of the glaciers. Thus, although spatial heterogeneity exhibits a predictable pattern in response to the seasonal flow regime, this pattern is likely to vary on a time-scale of a few years. For example, reconnection between floodplain channels and the river during the six-year flood on 29 June 1997 caused a 42% increase in surface hydrological connectivity (SC increased from 31 to 44% at a discharge of 6 m^3 s^{-1}). This increase in hydrological connectivity probably accounted for the lower evenness and thus diversity of specific conductance observed during the summer 1997. It also explains why the polynomial model proved to be more satisfactory when considering only post-flood data for specific conductance. We believe that the landscape indices employed in the present study are suitable for examining long-term changes in riverscape heterogeneity caused by glacial river channel evolution (Gurnell et al. 1999). In the Val Roseg catchment, riverscape heterogeneity (RH2) would fall below 1.5 in summer if 75% of the channel network was carrying dilute and turbid water. This may happen if the floodplain channel network becomes more braided in response to an increase in sediment delivery caused by erosive floods or the retreat of the glaciers.

Acknowledgements

We are indebted to P. Burgherr, R. Illi, B. Klein, D. Kistler, S. Meyns, B. Ribi, and T. Wellnitz for their professional and most dedicated help with the field and laboratory work. Special thanks to R. Zah for

his invaluable help with the mapping software. We also thank A. Papritz and D. Arscott for stimulating discussions and C. Robinson, U. Uehlinger, and 3 anonymous reviewers for their valuable critiques that improved the manuscript. We are grateful to Mr Testa and his crew at the Roseg Hotel for their hospitality and to the communes of Pontresina and Samedan for providing access to the sampling area. This work was supported by the Swiss National Science Foundation (SNF grant 21-49243.96).

References

Amoros, C. and Roux, A.L. 1988. Interaction between water bodies within the floodplains of large rivers: function and development of connectivity. *In* Connectivity in Landscape Ecology. pp. 125–130. Edited by K.L. Schreiber. Proc. 2nd Int. Seminar of the International Association for Landscape Ecology, Münstersche Geographische Arbeiten 29, Münster.

A.P.H.A. (ed.). 1989. Standard Methods for the Examination of Water and Wastewater. 17th ed., American Public Health Association, Washington.

Bayley, P.B. 1995. Understanding large river-floodplain ecosystems. BioScience 45: 153–158.

Bencala, K.E. 1993. A perspective on stream-catchment connections. J N Am Benthol Soc 12: 44–47.

Bonetto, C., de Cabo, L., Gabellone, N., Vinocur, A., Donadelli, J. and Unrein, F. 1994. Nutrient dynamics in the deltaic floodplain of the Lower Parana River. Arch Hydrobiol 131: 277–295.

Bornette, G. and Amoros, C. 1991. Aquatic vegetation and hydrology of a braided river floodplain. J Veg Sci 2: 497–512.

Burt, T.P. and Haycock, N.E. 1996. Linking hillslopes to floodplains. *In* Floodplain Processes. pp. 461–492. Edited by M.G. Anderson, E. Des Walling and P.D. Bates. John Wiley & Sons, New York.

Charles, D.F. (ed.). 1991. Acidic Deposition and Aquatic Ecosystems. Springer-Verlag, New York.

Chessel, D. and Dolédec, S. 1996. ADE software. Multivariate analyses and graphical display for environmental data. Université Claude Bernard Lyon I, Lyon.

Cooper, S.D., Barmuta, L., Sarnelle, O., Kratz, K. and Diehl, S. 1997. Quantifying spatial heterogeneity in streams. J N Am Benthol Soc 16: 174–188.

de Vries, J.J. 1995. Seasonal expansion and contraction of stream networks in shallow groundwater systems. J Hydrol 170: 15–26.

D.E.V. (ed.). 1985. Deutsche Einheitsverfahren zur Wasseruntersuchung. Verlag Chemie, Weinheim.

Dole, M.-J. 1983. Le domaine aquatique souterrain de la plaine alluviale du Rhône à l'Est de Lyon. 1. Diversité hydrologique et biocénotique de trois stations représentatives de la dynamique fluviale. Vie Milieu 33: 219–229.

Dolédec, S. and Chessel, D. 1987. Rythmes saisonniers et composantes stationnelles en milieu aquatique. I. Description d'un plan d'observations complet par projection de variables. Acta Œcol Gen 8: 403–426.

Dolédec, S. and Chessel, D. 1991. Recent developments in linear ordination methods for environmental sciences. Adv Ecol 1: 133–155.

Downes, M.T. 1978. An improved hydrazine reduction method for the automated determination of low nitrate levels in freshwater. Wat Res 12: 673–675.

Forsberg, B.R., Devol, A.H., Richey, J.E., Martinelli, L.A. and dos Santos, H. 1988. Factors controlling nutrient concentrations in Amazon floodplain lakes. Limnol Oceanogr 33: 41–56.

Furch, K. and Junk, W.J. 1993. Seasonal nutrient dynamics in an Amazonian floodplain lake. Arch Hydrobiol 128: 277–285.

Gregory, K.J. 1987. The hydrogeomorphology of alpine proglacial areas. *In* Glacio-fluvial sediment transfer. pp. 87–107. Edited by A.M. Gurnell and M.J. Clark. Wiley, Chichester.

Gurnell, A.M. and Clark, M.J. (eds). 1987. Glacio-fluvial sediment transfer. Wiley, Chichester.

Gurnell, A.M., Edwards P.J., Petts, G.E. and Ward, J.V. 1999. A conceptual model for alpine proglacial river channel evolution under changing climatic conditions. Catena 38: 223–242.

Gustafson, E.J. 1998. Quantifying landscape spatial pattern: what is the state of the art ? Ecosystems 1: 143–156.

Hamilton, S.K. and Lewis, W.M. 1987. Causes of seasonality in the chemistry of a lake on the Orinoco River floodplain, Venezuela. Limnol Oceanogr 32: 1277–1290.

Heiler, H., Hein, T., Schiemer, F. and Bornette, G. 1995. Hydrological connectivity and flood pulses as the central aspects for the integrity of a river-floodplain system. Regul Riv 11: 351–361.

Hoover, S.R. and Parker, A.J. 1991. Spatial components of biotic diversity in landscapes of Georgia, USA. Landsc Ecol 5: 125–136.

Juget, J., Amoros, C., Gamulin, D., Reygrobellet, J.-L., Richardot, M., Richoux, Ph. and Roux, C. 1976. Structure et fonctionnement des écosystèmes du Haut-Rhône Français. II. Etude hydrologique et écologique de quelques bras morts. Premiers résultats. Bull Ecol 7: 479–492.

Junk, W.J. 1997. The Central Amazon Floodplain. Springer, New York.

Junk, W.J., Bayley, P.B. and Sparks, R.E. 1989. The flood pulse concept in river-floodplain systems. *In* Proc. Int. Large River Symp. pp. 110–127. Edited by D.P. Dodge. Can Spec Publ Fish Aquat Sci 106.

Knowlton, M.F. and Jones, J.R. 1997. Trophic status of Missouri River floodplain lakes in relation to basin type and connectivity. Wetlands 17: 468–475.

Maizels, J.K. 1983. Proglacial channel systems: change and thresholds for change over long, intermediate and short time-scales. Spec Publ Int Assoc Sedimentol 6: 251–266.

Malard, F., Tockner, K. and Ward, J.V. 1999. Shifting dominance of subcatchment water sources and flow paths in a glacial flood plain (Val Roseg, Switzerland). Arct Antarct Alp Res 31: 135–150.

Milner, A.M. and Petts, G.E. 1994. Glacial rivers: physical habitat and ecology. Freshw Biol 32: 295–307.

O'Neill, R.V., Krummel, J.R., Gardner, R.H., Sugihara, G., Jackson, B., DeAngelis, D.L., Milne, B.T., Turner, M.G., Zygmunt, B., Christensen, S.W., Dale, V.H. and Graham, R.L. 1988. Indices of landscape pattern. Landsc Ecol 1: 153–162.

Parch, K., Jenik, J. and Large, A.R.G. (eds). 1996. Floodplain Ecology and Management, the Luznice River in the Trebon Biosphere Reserve, Central Europe. SPB Academic Publishing, Amsterdam.

Pielou, E.C. 1975. Ecological Diversity. Wiley, Chichester.

Robinson, C.T., Gessner, M.O. and Ward, J.V. 1998. Leaf breakdown and associated macroinvertebrates in alpine glacial streams. Freshw Biol 40: 215–228.

Romme, W.H. 1982. Fire and landscape diversity in subalpine forests of Yellowstone national park. Ecol Monogr 52: 199–221.

Roux, A.L. 1982. Cartographie polythématique appliquée à la gestion écologique des eaux. Etude d'un hydrosystème fluvial: le Haut-Rhône français. Centre National de la Recherche Scientifique, Paris.

Spreafico, M., Leibundgut, C. and Weingartner, R. 1992. Hydrological Atlas of Switzerland. Hydrological and Geological Swiss Survey, Bern.

Stanley, E.H., Fisher, S.G. and Grimm, N.B. 1997. Ecosystem expansion and contraction in streams. BioScience 47: 427–435.

Thioulouse, J. 1989. Statistical analysis and graphical display of multivariate data on the Macintosh. Comput Applic Biosc 5: 287–292.

Tockner, K., Malard, F., Burgherr, P., Robinson, C.T., Uehlinger, U., Zah, R. and Ward, J.V. 1997. Physico-chemical characterization of channel types in a glacial floodplain ecosystem (Val Roseg, Switzerland). Arch Hydrobiol 140: 433–463.

Tockner, K., Pennetzdorfer, D., Reiner, N., Schiemer, F. and Ward, J.V. 1999. Hydrological connectivity, and the exchange of organic matter and nutrients in a dynamic river-floodplain system (Danube, Austria). Freshw Biol 41: 521–535.

Trémolières, M., Eglin, I., Roeck, U. and Carbiener, R. 1993. The exchange process between river and groundwater on the Central Alsace floodplain (Eastren France). Hydrobiologia 254: 133–148.

Turner, M.G. and Gardner, R.H. 1991.Quantitative methods in landscape ecology: an introduction. *In* Quantitative Methods in Landscape Ecology. pp. 3–14. Edited by M.G. Turner and R.H. Gardner. Springer-Verlag, New York.

Turner, J.V. and Macpherson, D.K. 1990. Mechanisms affecting streamflow and stream water quality: an approach via stable isotope, hydrogeochemical, and time series analysis. Wat. Res Res 26: 3005–3019.

Uehlinger, U., Bossard, P., Bloesch, J., Bürgi, H.R., and Bührer, H. 1984. Ecological experiments in limnocorrals: methodological problems and quantification of the epilimnetic phosphorous and carbon cycles. Verh Int Verein Limnol 22: 163–171.

Uehlinger, U., Zah, R. and Bürgi, H.R. 1998. The Val Roseg project: temporal and spatial patterns of benthic algae in an alpine stream ecosystem influenced by glacier runoff. IAHS Publ 248: 419–424.

Van den Brink, F.W.B., de Leeuw, J.P.H.M., van der Velde, G. and Verheggen, G.M. 1993. Impact of hydrology on the chemistry and phytoplankton development in floodplain lakes along the Lower Rhine and Meuse. Biogeochemistry 19: 103–128.

Vogler, P. 1965. Beiträge zur Phosphoranalytik in der Limnologie. Fortschr Wasserchemie und Grenzgebiete 2: 109–119.

Ward, J.V. 1997. An expansive perspective of riverine landscapes: pattern and process across scales. Gaia 6: 52–60.

Ward, J.V. and Stanford, J.A. 1995. Ecological connectivity in alluvial river ecosystems and its disruption by flow regulation. Regul Riv 11: 105–119.

Ward J.V., Malard, F., Tockner, K. and Uehlinger, U. 1999. Influence of ground water on surface water conditions in a glacial flood plain of the Swiss Alps. Hydrol Process 13: 277–293.

Wiens, J.A. 1995. Landscape mosaics and ecological theory. *In* Mosaic landscapes and ecological processes. pp. 1–26. Edited by L. Hansson, L. Fahrig and G. Merriam. Chapman & Hall, London.